Decoherence-free quantum-information processing using dipole-coupled qubits

Peter G. Brooke[1,*]

[1]*Centre for Quantum Computer Technology and Department of Physics, Macquarie University, Sydney, New South Wales, Australia*

(Dated: February 1, 2008)

We propose a quantum-information processor that consists of decoherence-free logical qubits encoded into arrays of dipole-coupled qubits. High-fidelity single-qubit operations are performed deterministically within a decoherence-free subsystem without leakage via global addressing of bichromatic laser fields. Two-qubit operations are realized locally with four physical qubits, and between separated logical qubits using linear optics. We show how to prepare cluster states using this method. We include all non-nearest-neighbor effects in our calculations, and we assume the qubits are not located in the Dicke limit. Although our proposal is general to any system of dipole-coupled qubits, throughout the paper we use nitrogen-vacancy (NV) centers in diamond as an experimental context for our theoretical results.

PACS numbers: 03.67.Pp, 03.65.Yz, 03.67.Mn, 42.50.Fx

I. INTRODUCTION

In order to realize the promise of a quantum-information (QI) processor, the inevitable decoherence-inducing effect of any system-environment interaction must be taken into account. One method of doing this is to encode logical information into decoherence-free subsystems (DFSs) [1]. These are regions of the system Hilbert space that are not affected by any environment-induced nonunitary dynamics and which under certain conditions support perfect quantum memory.

The general formalism of DFS theory has been applied to a number of different physical systems, e.g., Ref. [2]. In this paper, we propose a quantum-information processor that consists of spatially separated arrays of three dipole-coupled qubits, each of which encodes a single DF qubit. Previous work of interest includes Petrosyan and Kurizki [3], in which the authors proposed local two-qubit operations that used two dipole-coupled qubits. Here, the physical qubits are also dipole-coupled. It is this coupling that is exploited in order to encode and rotate a DF qubit to high fidelity, and to enable cluster-state preparation. For the purposes of this paper, we focus on the dominant form of decoherence at small qubit separations: *strong-collective* decoherence. Fortunately, encoding to prevent this type of decoherence is scalable to N-qubit systems [4]. We show how to encode, manipulate without leakage, and read out QI from a DF qubit using only global control. We then show how to perform two-qubit operations and prepare a cluster state with the spatially separated qubit systems.

Complimenting theoretical progress, there have been experimental studies of DFSs, but, although there are many ways of processing QI, deterministically encoding, processing, and reading a single DF qubit is difficult. In ion traps, Kielpinski *et al.* used a DF state of two trapped ions to enable encoded information to be stored longer than its unencoded counterpart [5]. This DF state has also been prepared by Kwiat *et al.* in an optical system using parametric down conversion [6]. More recently, the same technique was used to prepare a strong-collective DF qubit from four physical qubits [7]. In liquid NMR, two physical qubits were used to demonstrate the Deutsch-Josza algorithm [8], with the antisymmetric collective state used to protect against decoherence. Also in NMR, Viola *et al.* [9] encoded a logical qubit into three nuclear spins in order to protect against collective noise. As well as realizing a similar encoding here, we also propose a method to rotate a logical qubit to high fidelity using only global control. Our results are relevant to any system that is described by a dipole-dipole interaction and, in light of recent experimental progress, are directly applicable to nitrogen-vacancy (NV) centers in diamond.

NV defects in diamond have been characterized extensively [10], and recently have been used for processing quantum information. In Ref. [11], high-fidelity one- and two-qubit operations in a single NV defect were demonstrated. There has also been a full quantum-process tomography of a qubit encoded in an NV defect [12]. Here, we apply results obtained from a general master-equation analysis to the evolution of three closely spaced dipole-coupled NV centers.

The paper is summarized as follows. In Sec. II we explicitly define a qubit, and describe a particular unraveling of the Lindblad master equation. Then in Sec. III we propose a method to deterministically prepare maximally entangled states in a three-qubit system, and give conditions that allow for preparation that is fast relative to the decoherence rate. In Sec. IV, we show how to transfer quantum information between the entangled states in a DFS, and in Sec. V we use the preparation method to read out the state of the encoded qubit. In Sec. VI we propose a method to perform local two-qubit operations in a system of NV centers, and then show how to prepare a cluster state with spatially separated systems of physical qubits using linear optics.

*Electronic address: pgb@ics.mq.edu.au

II. PHYSICAL SYSTEM

To support the proposed encoding three qubits are required. Although the qubits could be realized with any system that is described by a dipole-dipole interaction, we focus on NV centers in diamond. These can be manufactured [13], and consist of one singlet (^{1}A) and two triplet states (^{3}E and ^{3}A). Optical excitation and deexcitation is possible only between $\mathrm{m}_s = 0$ states [14]. Some deexcitation occurs to ^{1}A, but the effect of this level on the emission dynamics can be ignored [15]. So, a physical qubit consists of the electric-dipole transition $|1\rangle \equiv |^3\mathrm{E}, \mathrm{m}_s = 0\rangle$, and $|0\rangle \equiv |^3\mathrm{A}, \mathrm{m}_s = 0\rangle$.

For the theoretical analysis, this is equivalent to an electric-dipole coupled two-level system with resonant frequency ω_0 and half-linewidth γ. We assume that the spatial extent of the vacancy is much less than the resonant wavelength $\lambda_0 = 2\pi/k_0$, i.e., the qubits are effectively point dipoles. We describe the driving field as a classical bichromatic field that drives all three qubits simultaneously, but due to the small qubit-qubit separations cannot drive each qubit individually. Regarding NV centers, we assume that since they are closely spaced any cavity effects due to the diamond structure are ignored, and that any incident laser field on resonance with the physical qubits is off-resonant with all other parts of the diamond lattice. We assume that any inhomogeneous broadening of the electronic transition is small compared to ω_0 [16]. For this paper, we require aligned dipole moments. Fortunately, NV centers have only four orientations so, in the absence of any field, three NV centers will be aligned with probability $\frac{1}{64}$ [10].

Our analysis is in accordance with standard quantum optical methods for electric dipole-coupled qubits: a quantum master equation employing the rotating-wave and Born-Markov approximations. We assume that retardation effects can be ignored, which is valid provided that the separation of qubits i and j (quantified by their separation vector $\boldsymbol{r}_{ij}$) has a value of $\xi_{ij} \equiv k_0 r_{ij} \lesssim 1$ for unit vector $\vec{r}_{ij} = \boldsymbol{r}_{ij}/r_{ij}$ [17]. The raising operator for qubit i is $\hat{\sigma}_{i+} = |1\rangle_i\langle 0| = \hat{\sigma}_{i-}^\dagger$ and $\hat{\sigma}_{iz} = \frac{1}{2}[\hat{\sigma}_{i+}, \hat{\sigma}_{i-}]$. The transition-matrix element of the qubit is given by $\boldsymbol{d} = {}_i\langle 0|\,\hat{\boldsymbol{d}}_i\,|1\rangle_i$ with the dipole operator $\hat{\boldsymbol{d}}_i$ for qubit i. The dipoles of the three qubits are identically oriented, with $\vec{d}\cdot\vec{r}_{ij} = \cos\alpha$ for $\vec{d}$ the unit vector in direction $\boldsymbol{d}$. Since all the qubits are identical, the matrix elements of their dipole operators are equal: $\boldsymbol{d} = \boldsymbol{d}_i \forall i$.

The free evolution of three dipole-coupled qubits, including all non-nearest-neighbor interactions, without an incident field is ($\hbar = 1$) [18]

$$\widehat{H}_\mathrm{S} = \frac{\omega_0}{2}\sum_{i=1}^{3}\hat{\sigma}_{iz} + \sum_{i\neq j=1}^{3}\Xi_{ij}\hat{\sigma}_{i+}\hat{\sigma}_{j-} - \mathrm{i}\frac{\gamma}{2}\sum_{i=1}^{3}\hat{\sigma}_{i+}\hat{\sigma}_{i-}, \tag{1}$$

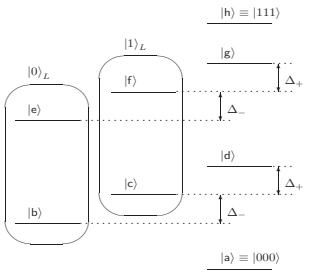

FIG. 1: Energy-level scheme of three qubits, with $\Delta_\pm = -\Delta_{13} \pm \frac{1}{2}(\Delta_{13} + \Omega)$, for $\Omega \equiv \sqrt{8\Delta_{12}^2 + \Delta_{13}^2}$. In the Dicke limit [19], $|\mathsf{b}\rangle \equiv \frac{1}{\sqrt{6}}(-2\,|001\rangle + |010\rangle + |100\rangle)$ and $|\mathsf{c}\rangle \equiv \frac{1}{\sqrt{2}}(|010\rangle - |100\rangle)$. The DFS is labeled $\{|0\rangle_L, |1\rangle_L\}$ [4].

with

$$\Xi_{ij} \equiv -\frac{3\gamma}{4}\frac{\mathrm{e}^{\mathrm{i}\xi_{ij}}}{\xi_{ij}^3}\left[\xi_{ij}^2\sin^2\alpha - (1-\mathrm{i}\xi_{ij})\left(1-3\cos^2\alpha\right)\right] \tag{2}$$

for $i, j = 1, 2, 3$, and $\xi_{ij} \equiv k_0 r_{ij}$. By symmetry, $\Xi_{ij} = \Xi_{ji}$, and we define $\Delta_{ij} \equiv \mathrm{Re}\{\Xi_{ij}\}$ and $\gamma_{ij} \equiv -2\,\mathrm{Im}\{\Xi_{ij}\}$. The coefficients Δ_{ij} and γ_{ij} correspond to the static dipole-dipole interaction and the actual process of photon emission respectively. We label the energy levels in order of increasing energy: $\mathsf{a}, \ldots, \mathsf{h}$ (see Fig. 1).

The laser has a bichromatic electric field $\boldsymbol{E}(\boldsymbol{r}) = \boldsymbol{E}_\mu(\boldsymbol{r}) + \boldsymbol{E}_\nu(\boldsymbol{r})$, with $\boldsymbol{E}_\mu(\boldsymbol{r})$ and $\boldsymbol{E}_\nu(\boldsymbol{r})$ the electric field amplitudes. $\boldsymbol{E}(\boldsymbol{r})$ interacts with the three qubits via a dipole coupling and so we introduce the Rabi frequencies $\mathcal{E}_{\mu,i} = \vec{d}\cdot\boldsymbol{E}_\mu \mathrm{e}^{-\mathrm{i}\boldsymbol{k}_\mu\cdot\boldsymbol{r}_i}$ and $\mathcal{E}_{\nu,i} = \vec{d}\cdot\boldsymbol{E}_\nu \mathrm{e}^{-\mathrm{i}\boldsymbol{k}_\nu\cdot\boldsymbol{r}_i}$ for wave vectors $\boldsymbol{k}_\mu$ and $\boldsymbol{k}_\nu$, and where qubit i is situated at $\boldsymbol{r}_i$. Within the rotating-wave approximation, the interaction Hamiltonian is written

$$\widehat{H}_\mathrm{I} = \sum_{i=1}^{3}\mathcal{E}_i\hat{\sigma}_{i-} + \mathrm{H.c.}, \tag{3}$$

for which $\mathcal{E}_i$ are copropagating and described by a time-dependent bichromatic external field,

$$\mathcal{E}_i = \mathcal{E}_{\mu,i}\mathrm{e}^{-\mathrm{i}\omega_\mu t} + \mathcal{E}_{\nu,i}\mathrm{e}^{-\mathrm{i}\omega_\nu t}. \tag{4}$$

Due to the different positions of the qubits, the field $\mathcal{E}_i$ differs for distinct qubits. The total effective Hamiltonian for the no-jump evolution is $\widehat{H}_\mathrm{eff} = \widehat{H}_\mathrm{S} + \widehat{H}_\mathrm{I}$.

The jump operators are identified by diagonalizing the relaxation matrix (γ_{ij}) [20],

$$(\gamma_{ij}) = \boldsymbol{B}^T\boldsymbol{\Lambda}\boldsymbol{B}, \tag{5}$$

where $\boldsymbol{\Lambda} \equiv \mathrm{diag}\,(\lambda_1, \lambda_2, \lambda_3)$ is a diagonal matrix of the eigenvalues of (γ_{ij}) and the columns of $\boldsymbol{B}^T = (b_{ij})^T$,

$$\boldsymbol{b}_l = \begin{pmatrix} b_{l1} \\ b_{l2} \\ b_{l3} \end{pmatrix} \tag{6}$$

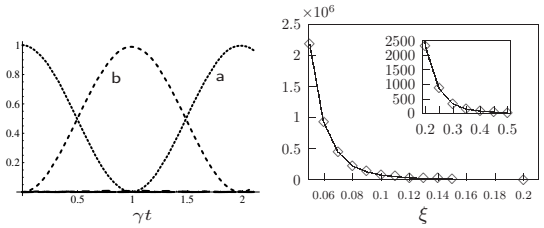

(a) (b)

FIG. 2: (a) Population of the levels $\mathsf{a},\ldots,\mathsf{h}$ for $\xi_{12} = 0.5$, $\mathcal{E}_\mu = \gamma$, $\omega_\mu = \frac{1}{2}(\Delta_{13} - \Omega)$, and $\alpha = 0$. For these parameters, $F = 0.988$ and the time taken for the transfer a-b: $t_\pi = 0.987\gamma^{-1}$. (b) Number of population inversions possible during time period γ_b^{-1} versus qubit separation with $F = 0.98$ and $\alpha = 0$. For the separation proposed in Ref. [23], $\gamma_\mathsf{b} t_\pi \approx 5 \times 10^{-7}$.

are the corresponding normalized eigenvectors. We define $\widehat{\mathbf{\Sigma}}^\dagger \equiv (\widehat{\sigma}_{1+}, \widehat{\sigma}_{2+}, \widehat{\sigma}_{3+})$, so the jump operators are written

$$\widehat{J}_l = \sqrt{\lambda_l}\boldsymbol{b}_l^T\widehat{\mathbf{\Sigma}} \qquad \text{and} \qquad \widehat{J}_l^\dagger = \sqrt{\lambda_l}\widehat{\mathbf{\Sigma}}^\dagger\boldsymbol{b}_l. \tag{7}$$

These are quoted explicitly for three qubits in Ref. [20]. In this unraveling, the master equation is

$$\dot{\hat{\rho}} = -\frac{\mathrm{i}}{\hbar}(\widehat{H}_{\rm eff}\hat{\rho} - \hat{\rho}\widehat{H}_{\rm eff}^\dagger) + \sum_{i=1}^{3}\widehat{J}_i\hat{\rho}\widehat{J}_i^\dagger, \tag{8}$$

which corresponds to the standard Lehmberg master equation for three qubits [21] and is simply the Lindblad master equation [22]. This unraveling is useful for analyzing preparation, manipulation, and read out of DFS-encoded quantum information in dipole-coupled qubits.

III. PREPARATION

We describe how to prepare the maximally entangled DFS state $|\mathsf{b}\rangle$ deterministically. This state is the lower state of $|0\rangle_L$, and is the longest-lived excited state in the eight-level system. For the purposes of preparation, we require only a single laser field,

$$\widehat{H}_{\rm I} = \sum_{i=1}^{3}\mathcal{E}_{\mu,i}\mathrm{e}^{-\mathrm{i}\omega_\mu t}\widehat{\sigma}_{i-} + \text{H.c.}, \tag{9}$$

with frequency ω_μ, and $\boldsymbol{k}_\mu$ orthogonal to the line joining the qubits. We assume that the initial state is the ground state and that the qubits are positioned according to $\boldsymbol{r}_1 = -\boldsymbol{r}$, $\boldsymbol{r}_2 = 0$, and $\boldsymbol{r}_3 = \boldsymbol{r}$. Under these conditions, in the interaction picture with respect to the Hermitian part of $\widehat{H}_{\rm S}$, the effective coupling between states $|\mathsf{a}\rangle$ and $|\mathsf{b}\rangle$ in the collective basis is

$$\mathcal{E}_{\rm eff} = \frac{1}{\Omega}\sqrt{\frac{\Omega}{\kappa}}\mathcal{E}_\mu(\kappa\cos\boldsymbol{k}_\mu r - 2\Delta_{12}), \tag{10}$$

where $\mathcal{E}_\mu = |\mathcal{E}_{\mu,i}|$, $\kappa \equiv \Omega - \Delta_{13}$, and Ω is defined in Fig. 1. In Eq. (10) we have chosen $\omega_\mu = \frac{1}{2}(\Delta_{13} - \Omega)$, so that $\mathcal{E}_{\rm eff}$ is resonant with the a-b transition.

To ensure $|\mathsf{b}\rangle$ is prepared to high fidelity, $\Omega \gg \gamma$. Due to the divergence of the dipole-dipole interaction, this is naturally satisfied at qubit separations small compared to λ_0. For an NV center in diamond, the separation between qubits for the purposes of preparation is assumed to be $r = 50$nm, or $\xi_{12} = 0.5$. This is within the capabilities of present technology. In fact, there are proposals for $r \approx 1$nm with the position of the qubit known to sub-nm accuracy [23].

The effect of the laser taking into account the full eight-level Hamiltonian (assuming no photon emission) has been determined numerically [see Fig. 2(a)]. To quantify the success of the transfer a-b, we use fidelity (F) as a distance measure [24]. In order to maintain high fidelity, the Rabi frequency $\mathcal{E}_\mu$ cannot be made arbitrarily large. This is because the coupling $\mathcal{E}_{\mathsf{ad}} \propto \mathrm{e}^{\mathrm{i}\Omega t}$. So, increasing $\mathcal{E}_\mu$ without altering Ω means the coupling a-d will no longer be rapidly oscillating compared to the coupling a-b [Eq. (10)]. Note also that $\mathcal{E}_{\mathsf{ac}} \propto \mathrm{e}^{\mathrm{i}\Omega t}$, but since the magnitude of the coupling a-c is much less than the magnitude of the coupling a-d, a-c is weakly coupled compared to a-d.

We now focus our attention on the robustness of the preparation to variations in Rabi frequency, detuning, and separation (see Table I). We assume the Rabi frequency is equal to some value $\mathcal{E}$, rather than $\mathcal{E}_\mu = \gamma$. The fidelity of the preparation after time t_π—the time taken for population inversion—remains high, even for $\mathcal{E}/\mathcal{E}_\mu = \frac{3}{4}$. Thus, preparation is robust to small variations in $\mathcal{E}_\mu$. For detuning, we assume the laser frequency equals some value ω, rather than ω_μ. For separation, we assume that in practice there will always be some uncontrollable variation in qubit separation, so the positions of the qubits are known only to a certain error. However, once they are positioned, they do not move. This is peculiar to NV centers in diamond and may not apply to other physical implementations of our proposal (e.g., atom traps). We assume that the probability distribution of the position of qubit i is a Gaussian with mean zero and variance v in units of λ_0 centered at $\boldsymbol{r}_i$. The position of the qubit is taken from this distribution using Monte Carlo techniques. Table I shows the limits on separation inaccuracy, averaged over 100 different initial positions.

	$F > 0.90$	$F > 0.95$	$F > 0.98$
Rabi frequency, $\mathcal{E}_\mu$	$\pm 20\%$	$\pm 12.5\%$	$\pm 6\%$
Detuning, ω_μ	$\pm 5\frac{1}{2}\%$	$\pm 4\%$	$\pm 1\frac{1}{2}\%$
Position variance, v		0.08	0.005

TABLE I: Level of control for preparation of $|\mathsf{b}\rangle$ for exact values quoted in Fig. 2(a) with variance v. For $F > 0.9$, the overlap of the distribution of the position of two NV centers is large, causing their order to change. This renders a value for v meaningless.

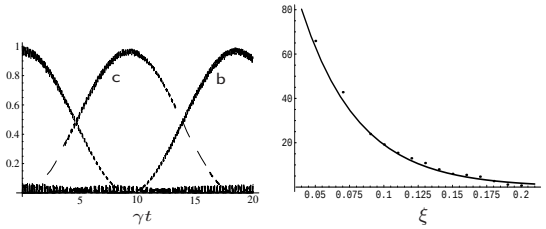

(a) (b)

FIG. 3: (a) Population of the levels $\mathsf{a},\ldots,\mathsf{h}$ with $\xi_{12}=0.15$, $\mathcal{E}_\mu=6\gamma$, $\mathcal{E}_\nu=15\gamma$, $\omega_\delta=170\gamma$, and $\alpha=\frac{\pi}{2}$. For these parameters, $F=0.986$ and the time taken for the transfer b-c: $t_\pi=9.271\gamma^{-1}$. (b) Number of qubit rotations b-c possible during time period $\frac{1}{2}(\gamma_\mathsf{b}+\gamma_\mathsf{c})^{-1}$ versus qubit separation with $F=0.98$ and $\alpha=\frac{\pi}{2}$.

If proposal [23] is implemented, then typical variations of the NV centers will be ∼nm, which is $\sim 0.0015\lambda_0$, the frequency of typical lasers can be controlled to within one part in 10^8, and their amplitude varies by less than 0.25% every 10 seconds [25]. So, in light of Table I high-fidelity preparation in NV centers, although certainly an experimental challenge, is possible with present technology.

Before describing our method to rotate a DFS qubit, we explicitly include the probability of decay. The imaginary part of the eigenvalues of Eq. (1) give the linewidths of the eigenstates. The linewidth of $|\mathsf{b}\rangle$, γ_b, decreases with decreasing qubit separation. Thus, we examine the number of population inversions possible in time period γ_b^{-1} with respect to physical qubit separation [see Fig. 2(b)]. This improves dramatically for small separations.

IV. LOGICAL QUBIT ROTATION

In order to rotate the encoded qubit, we use a bichromatic laser field. With the appropriate laser detunings this causes population between $|\mathsf{b}\rangle$ and $|\mathsf{c}\rangle$ to undergo coherent oscillations, without populating other eigenstates. At nonzero separation the DFSs are mixed by spontaneous emission, so in order to ignore this effect, we choose the lowest-energy states. The laser frequencies are chosen so that

$$\omega_\mu=\omega_\delta \qquad \text{and} \qquad \omega_\nu=\tfrac{1}{2}(3\Delta_{13}-\Omega)+\omega_\delta, \tag{11}$$

where ω_μ (ω_ν) is resonant with transition b-e(c-e). Similar to a two-photon Raman transition in an isolated three-level system, ω_μ and ω_ν are detuned from resonance by ω_δ. The effective couplings for the transitions b-e and c-e are

$$\mathcal{E}_{\mathsf{be}}=\frac{1}{2\Omega}\mathrm{e}^{-\frac{\mathrm{i}}{2}(\eta-2\omega_\delta)t}(\mathrm{e}^{\frac{\mathrm{i}}{2}\eta t}\mathcal{E}_\mu+\mathcal{E}_\nu)(\kappa-8\Delta_{12}\cos\boldsymbol{k}r) \tag{12}$$

	$F>0.90$	$F>0.95$	$F>0.98$
Rabi frequency, $\mathcal{E}_\mu\mathcal{E}_\nu/90$	±12%	±8%	±1%
Detuning, ω_δ	±28%	±18%	±6%
Position variance, v	1.6×10^{-3}	0.8×10^{-3}	6×10^{-6}

TABLE II: Level of control for oscillations between b-c for exact values quoted in Fig. 3(a) with variance v.

and

$$\mathcal{E}_{\mathsf{ce}}=\sqrt{\frac{2\kappa}{\Omega}}\frac{\Delta_{12}\eta}{\Omega^2-\Delta_{13}(\Delta_{13}+4\kappa)}\mathrm{e}^{-\mathrm{i}(\boldsymbol{k}r-\omega_\delta t)} \times(1-\mathrm{e}^{2\mathrm{i}\boldsymbol{k}r})(\mathrm{e}^{\frac{\mathrm{i}}{2}\eta t}\mathcal{E}_\mu+\mathcal{E}_\nu) \tag{13}$$

for $\boldsymbol{k}$ orthogonal to the line joining the qubits with $\boldsymbol{k}_\mu=\boldsymbol{k}_\nu=\boldsymbol{k}$, and for $\eta\equiv\Omega-3\Delta_{13}$.

Consider the three-level system b-c-e in isolation, with the couplings calculated from $\widehat{H}_\mathrm{I}$. After adiabatically eliminating $|\mathsf{e}\rangle$, the effective Rabi frequency between $|\mathsf{b}\rangle$ and $|\mathsf{c}\rangle$ in the collective basis and interaction picture is

$$\mathcal{E}_\mathrm{eff}=\frac{\mathrm{e}^{-\mathrm{i}(\boldsymbol{k}r+t\eta)}\kappa^{3/2}}{4\sqrt{2}\omega_\delta(\kappa\Delta_{13}-2\Delta_{12}^2)^2\Omega^{3/2}}(\mathrm{e}^{2\mathrm{i}\boldsymbol{k}r}-1)\Delta_{12} \times\eta(\mathrm{e}^{\frac{\mathrm{i}}{2}t\eta}\mathcal{E}_\mu+\mathcal{E}_\nu)(\mathcal{E}_\mu+\mathrm{e}^{\frac{\mathrm{i}}{2}t\eta}\mathcal{E}_\nu) \times(2\Delta_{12}^2-\Delta_{13}\kappa-2\Delta_{12}\eta\cos\boldsymbol{k}r). \tag{14}$$

In order to calculate the detuning from resonance, ω_δ, the level shift caused by the interaction of the laser with the qubits was included. This was done numerically. We calculate the population (assuming no photon emission) of all eight states for the initial state $|\mathsf{b}\rangle$ [see Fig. 3(a)].

The effective Rabi frequency cannot be made arbitrarily large: this causes population excitation into $|\mathsf{e}\rangle$ and $|\mathsf{f}\rangle$, and, if the increase is large enough, transitions into $|\mathsf{h}\rangle$. If $\mathcal{E}_{\mu(\nu)}\gg\mathcal{E}_{\nu(\mu)}$, then the population will oscillate between b-e (c-e). In order for the adiabatic elimination of the upper state e to remain valid, $\mathcal{E}_\mathrm{eff}\ll\omega_\delta$. We examine the robustness of the logical qubit rotations to variations in Rabi frequency, detuning, and separation. For the Rabi frequency, we simultaneously vary $\mathcal{E}_\mu$ and $\mathcal{E}_\nu$ away from the exact values and examine F at t_π, all of which are quoted in Fig. 3(a). We examine the ratio $\mathcal{E}_\mu\mathcal{E}_\nu/90$ for $\mathcal{E}_\mu,\mathcal{E}_\nu$ chosen close to the values in Fig. 3(a) (see Table II). For high-fidelity rotations, the level of control of the Rabi frequency is high, but due to the small separation, greater tolerance for the detuning is permitted. Regarding NV centers, high-fidelity rotations are possible with sub-nm position control [23]. Note that this control assumes that once the NV centers are located, their positions cannot be determined, and so the frequencies of the control fields cannot be adjusted accordingly.

The number of rotations possible in a single spontaneous emission lifetime enables us to see the gains obtained from using DFS encoding. For the linewidth of the qubit we use $\frac{1}{2}(\gamma_\mathsf{b}+\gamma_\mathsf{c})$, which is the average linewidth

of the two states. Figure 3(b) shows the number of qubit rotations per spontaneous emission lifetime. As the separation increases, the number of rotations decreases. This is partly due to the increase in linewidth with increasing separation, but mainly due to $\Delta_\pm$ decreasing in size. This means the three-level system b-c-e can no longer be treated in isolation. In fact,

$$\lim_{\xi_{ij}\to\infty} \mathcal{E}_{\text{eff}} = 0. \tag{15}$$

At separations much larger than $\xi = 0.2$, or 20nm, the time taken for the rotation is above that taken for decay from b and c, negating the benefits of the proposed DFS encoding for quantum-information processing.

V. STATE READ OUT

This is performed in a similar way to preparation. We exploit the splitting of the eigenbasis in order to isolate a one-photon transition that will fluoresce if populated. For this purpose, a single laser field is required [see Eq. (9)]. Similar to preparation, the detuning of the laser field is chosen to be equal to $\omega_\mu = \frac{1}{2}(3\Delta_{13}+\Omega)$. So, the (resonant) coupling between states $|\mathsf{c}\rangle$ and $|\mathsf{g}\rangle$ is:

$$\mathcal{E}_{\mathsf{cg}} = \frac{\mathrm{i}}{\sqrt{2}}\sqrt{1+\frac{\Delta_{13}}{\Omega}}\frac{\Delta_{12}(\Omega+3\Delta_{13})\mathcal{E}_\mu \sin \boldsymbol{k}r}{2\Delta_{12}^2+\Delta_{13}(\Omega+\Delta_{13})}. \tag{16}$$

If the qubit is in $|1\rangle_L$, then fluorescence will be detected, if not, then the system will remain dark. The decay width of state $|\mathsf{g}\rangle$ is

$$\gamma_{\mathsf{g}} = \frac{1}{2}\left(4\gamma+\gamma_{13}+\sqrt{8\gamma_{12}^2+\gamma_{13}^2}\right). \tag{17}$$

This is superradiant with an upper bound of 4γ. In order to read out $|0\rangle_L$, the frequency of the laser field is chosen to be resonant with the transition b-g, i.e., $\omega_\mu = \Omega$.

VI. TWO-QUBIT OPERATIONS AND CLUSTER-STATE PREPARATION

In order to perform an arbitrary sequence of quantum logic operations two-qubit entangling operations are required [24]. Here, two methods of performing these operations are described. The first is a natural extension of Sec. IV, and the second applies the technique described in Ref. [27] to a collection of systems of three closely spaced physical qubits in order to prepare a cluster state.

A. Two-qubit operations

The smallest number of physical qubits that supports two decoherence-free qubits is four. The decoherence-free qubits are encoded into a decoherence-free subsystem and a decoherence-free subspace. Using the Dicke decomposition, the decoherence-free subspace in four qubits is [4]

$$|0\rangle_L = \frac{1}{2}(|01\rangle - |10\rangle)(|01\rangle - |10\rangle), \tag{18}$$

$$|1\rangle_L = \frac{1}{\sqrt{12}}(2\,|0011\rangle + 2\,|1100\rangle - |0101\rangle - |1010\rangle - |0110\rangle - |1001\rangle). \tag{19}$$

The Hilbert space is decomposed into irreducible representations: $\mathcal{H}_1 \oplus \mathcal{H}_1 \oplus \mathcal{H}_3 \oplus \mathcal{H}_3 \oplus \mathcal{H}_3 \oplus \mathcal{H}_5$, where the subscript labels the dimension. The decoherence-free subspace qubit is encoded across $\mathcal{H}_1 \oplus \mathcal{H}_1$, and the decoherence-free subsystem qubit across $\mathcal{H}_3 \oplus \mathcal{H}_3$.

The controlled-phase (CPHASE) gate, $\{|00\rangle_L, |01\rangle_L, |10\rangle_L, |11\rangle_L\} \to \{|00\rangle_L, |01\rangle_L, |10\rangle_L, -|11\rangle_L\}$, is an entangling operation. So that two qubits will yield two logical bits of information, the logical states are defined in pairs: $|\mathsf{b}\rangle \equiv |01\rangle_L$, $|\mathsf{c}\rangle \equiv |00\rangle_L$, $|\mathsf{f}\rangle \equiv |11\rangle_L$, $|\mathsf{g}\rangle \equiv |10\rangle_L$, where the Hilbert space is labeled a,b, ...,o,p in order of increasing energy. Using this labeling, a CPHASE operation is performed using a 2π pulse, off resonant with transition f-l, that produces a phase shift of -1. Arbitrary one-qubit operations are performed on the first qubit by resonantly coupling b-f and c-g simultaneously, and on the second qubit by rotating b-c and f-g using collective two-photon Raman transitions as described in Sec. IV.

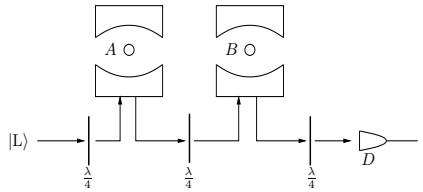

FIG. 4: CPHASE gate detailed in Ref. [27] between atom A and atom B. The $\frac{1}{4}$-wave plates are labeled with $\frac{\lambda}{4}$, and the polarization detector with D. A left-circularly polarized photon $|\mathrm{L}\rangle$ is input at the left, and the subsequent polarization is measured at D.

B. Cluster-state preparation

Although the previous method supports two-qubit operations, it is not conducive to QI processing in large systems: the entangling gate works only with isolated systems of neighboring qubits. One method that enables arbitrary quantum-logic operations is one-way computation [26]. In order to generate the cluster states required for this, we apply the method proposed in Cho and Lee [27] to a collection of spatially separated arrays of three dipole-coupled qubits that are situated in cavities.

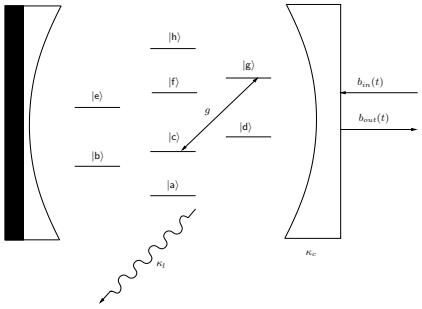

FIG. 5: The decoherence-free qubit is trapped in a one-sided optical cavity. The transition c-g is coupled resonantly to the right circularly polarized mode of the cavity with coupling constant g. The cavity photon is either transmitted through the cavity mirror with rate κ_c or lost with rate κ_l. $b_{in}(t)$ and $b_{out}(t)$ denote the input and output field operators, respectively.

In Ref. [27], the (atomic) qubit consists of the lower levels of a three-level atom (3LA), and is situated in a one-sided optical cavity. The right circularly polarized mode of the cavity photon resonantly couples one of the logical states (e.g., $|1\rangle$) to the upper state of the 3LA, but not the other. The phase of a right circularly polarized photon on exiting the cavity is unchanged if the qubit is in $|1\rangle$, otherwise the photon, whether right or left circularly polarized, acquires a π-phase shift. A CPHASE gate between two separated atomic qubits can be realized using the setup shown in Fig. 4.

This system can be realized here by placing the logical qubit inside a cavity (see Fig. 5). The encoded qubit is placed in a cavity on resonance with $\frac{1}{2}(3\Delta_{13}+\Omega)$ so only the right circularly polarized cavity photon interacts with the qubit in state $|\mathsf{c}\rangle$. If the qubit is in $|\mathsf{b}\rangle$, the cavity photon acquires a π-phase shift, otherwise it does not. Then, two-qubit operations are performed in the same manner as described in Ref. [27].

However, our setup has a number of further requirements. First, the atom-cavity coupling rate has to be fast compared to the decay time scale of the DF state $|\mathsf{c}\rangle$. Second, $|\mathsf{g}\rangle$ is superradiant [Eq. (17)], so the atom-cavity coupling rate must be fast compared to γ_{g}. Fortunately, the upper bound of γ_{g} is 4γ, which is small compared to $\Delta_{\pm}$. Third, as well as the probability of logical qubit decay, if there is a decay from g, the most probable decay channel is g-d not g-c, so any decay implies information loss.

Cluster states can be generated as follows [27]. The 1D cluster state of N qubits can be written as

$$|\Psi_N\rangle = \frac{1}{\sqrt{2}}|\phi_0\rangle_{N-3}|0\rangle_{N-2}\left(|0\rangle_{N-1}|+\rangle_N + |1\rangle_{N-1}|-\rangle_N\right) + \frac{1}{\sqrt{2}}|\phi_1\rangle_{N-3}|1\rangle_{N-2}\left(|0\rangle_{N-1}|+\rangle_N - |1\rangle_{N-1}|-\rangle_N\right) \quad (20)$$

for $|\pm\rangle = \frac{1}{\sqrt{2}}(|0\rangle \pm |1\rangle)$, where the subscript labels the qubit, and the terms for the $(N-3)$ qubits are denoted by $|\phi_i\rangle$. The state $|\Psi_{N+1}\rangle$ can be generated by attaching a qubit in $|+\rangle$ to $|\Psi_N\rangle$ by performing a CPHASE operation. If this operation fails, state (20) becomes a mixed state. However, $|\Psi_{N-2}\rangle$ can be recovered from this state by measuring the $(N-1)$th qubit in the computational basis and performing an operation on the $(N-2)$nd qubit dependent on the measurement result. The average number of qubits attached to the cluster state by m CPHASE operations is $(3P-2)m$, which grows if $P > 2/3$. So, cluster states consisting of DF logical qubits inside separate cavities can be prepared to high-fidelity using linear optics.

VII. CONCLUSION

We have proposed a general method to prepare a maximally entangled DFS state in a linear array of dipole-coupled qubits that, although relevant to any system of dipole-coupled qubits, in the light of recent experimental progress, is directly applicable to a system of NV centers in diamond. The preparation is possible to high-fidelity, and can be performed quickly relative to the linewidth of the entangled state. We showed how to rotate a logical qubit to high-fidelity within a DFS without leakage, and quickly relative to the combined decay of the logical states. Similar to the preparation, we showed how to read out a logical state with high-fidelity. We then described two methods to perform two-qubit operations, one of which enables cluster-state preparation in a system of spatially separated DF dipole-coupled qubits.

Acknowledgments

We especially thank Karl-Peter Marzlin for many helpful discussions. We also thank Jim Cresser, Barry Sanders, and Jason Twamley for comments on the manuscript. This work was supported by Macquarie University.

[1] G.M. Palma, K.-A. Suominen, and A. K. Ekert, Proc. Roy. Soc. London Ser. A, **452**, 567 (1996); L.-M Duan and G.-C. Guo, Phys. Rev. Lett. **79**, 1953 (1997); P. Zanardi and M. Rasetti, *ibid.* **79**, 3306 (1997); D.A. Lidar, I. L. Chuang, and K. B. Whaley, *ibid.* **81**, 2594 (1998); E. Knill, R. Laflamme, and L. Viola, *ibid.* **84**, 2525 (2000).

[2] A. Beige, D. Braun, B. Tregenna, and P. L. Knight, Phys. Rev. Lett. **85**, 1762 (2000); M. Feng and X. Wang, Phys. Rev. A **65**, 044304 (2002); P. Zanardi and F. Rossi, Phys. Rev. Lett. **81**, 4752 (1998).

[3] D. Petrosyan and G. Kurizki, Phys. Rev. Lett. **89**, 207902 (2002).

[4] J. Kempe, D. Bacon, D. A. Lidar, and K. B. Whaley, Phys. Rev. A **63**, 042307 (2001).

[5] D. Kielpinski *et al.*, Science **291**, 1013 (2001).

[6] P. G. Kwiat, A. J. Berglund, J. B. Altepeter, and A. G. White, Science **290**, 498 (2000).

[7] M. Bourennane, M. Eibl, S. Gaertner, C. Kurtsiefer, A. Cabello, and H. Weinfurter, Phys. Rev. Lett. **92**, 107901 (2004).

[8] M. Mohseni, J. S. Lundeen, K. J. Resch, and A. M. Steinberg, Phys. Rev. Lett. **91**, 187903 (2003).

[9] L. Viola *et al.*, Science **293**, 2059 (2001).

[10] G. Davies, *Properties and growth of diamond* (IEE/INSPEC, London, 1994), Vol. **9**.

[11] F. Jelezko *et al.*, Phys. Rev. Lett. **93**, 130501 (2004).

[12] M. Howard *et al.*, New J. Phys. **8**, 33 (2006).

[13] J. Meijer *et al.*, Appl. Phys. Lett. **87**, 261909 (2005); J.R. Rabeau *et al.*, *ibid.* (to be published).

[14] A.P. Nizovtsev *et al.*, Opt. Spectrosc. **94**, 848 (2003); Physica B **340**, 106 (2003).

[15] A. Drabenstedt *et al.*, Phys. Rev. B **60**, 11503 (1999).

[16] C. Santori *et al.*, Opt. Express **14**, 7986 (2006).

[17] P. W. Milonni and P. L. Knight, Phys. Rev. A **10**, 1096 (1974).

[18] H.J. Carmichael, *An Open Systems Approach to Quantum Optics* (Springer-Verlag, Berlin, 1993).

[19] R.H. Dicke, Phys. Rev. **93**, 99 (1954).

[20] J. P. Clemens, L. Horvath, B. C. Sanders, and H. J. Carmichael, Phys. Rev. A **68**, 023809 (2003).

[21] A.A. Belavkin *et al.*, Sov. Phys. JETP **56**, 264 (1969); G.S. Agarwal, Phys. Rev. A **2**, 2038 (1970); R.H. Lehmberg, *ibid.* **2**, 883 (1970); **2** 889 (1970).

[22] G. Lindblad, Commun. Math. Phys. **48**, 119 (1976)

[23] J. Meijer *et al.*, Appl. Phys. A **83**, 321 (2006).

[24] M.A. Nielsen and I.L. Chuang, *Quantum Computation and Quantum Information* (Cambridge University Press, Cambridge, England, 2000).

[25] See, e.g., the specifications published by the manufacturers New Focus at http://www.newfocus.com.

[26] H.J. Briegel and R. Raussendorf, Phys. Rev. Lett. **86**, 910 (2001); R. Raussendorf and H.J. Briegel, *ibid.* **86**, 5188 (2001).

[27] J. Cho and H.-W. Lee, Phys. Rev. Lett. **95**, 160501 (2005).